CONF-901025--34

CONF-901025--34

DE91 005490

High Density Regimes and Beta Limits in JET

by

The JET Team*
(presented by P Smeulders)

JET Joint Undertaking, Abingdon,
Oxon, OX14 3EA,UK.

* See : P-H.Rebut et al, 13th Int.Conf. on Plasma Physics and Contr. Nucl. Fusion Research, Washington (1990), to be published in Nuclear Fusion Supplement. Including the following: H.Goedbloed and G.Huysmans: FOM-Instituut voor Plasma Fysica, Nieuwegein, NL; and T.C Hender and O.J.Kwon,: UKAEA/ EURATOM Fusion Association, Culham Laboratory, UK.

High Density Regimes and Beta Limits in JET

Abstract

Results are first presented on the density limit in JET discharges with graphite (C), Be gettered graphite and Be limiters. There is a clear improvement in the case of Be limiters. The Be gettered phase showed no increase in the gas fuelled density limit, except with Ion Cyclotron Resonance Heating (ICRH), but, the limit changed character. During MARFE-formation, any further increase in density was prevented, leading to a soft density limit. The soft density limit was a function of input power and impurity content with a weak dependence on q. Helium and pellet fuelled discharges exceeded the gas-fuelled global density limits, but essentially had the same edge limit. In the second part, results are presented of high β operation in low-B Double-Null (DN) X-point configurations with Be-gettered carbon target plates. The Troyon limit was reached during H-mode discharges and toroidal β values of 5.5% were obtained. At high beta, the sawteeth were modified and characterised by very rapid heat-waves and fishbone-like pre- and post-cursors with strongly ballooning character.

1. OPERATION NEAR THE DENSITY LIMIT

Operation near the density limit has been systematically studied in JET for limiter discharges, with C limiters, with evaporated Be layers and with Be limiters [1]. The operating density in tokamaks is usually presented in the form given in Fig.1. Each point represents the maximum obtained normalised density during a discharge with either Ohmic (OH), Neutral Beam (NBI), ICRH or combined heating. The broken lines marked by OH (C) and NBI(C) are the highest limits obtained in the previous campaigns with C walls and limiters [2] ($nRq_\psi/B_t = 12$ for OH and $20\times10^{19}m^{-2}T^{-1}$ with NBI). There are clear improvements due to the Be limiters and Be coated walls. After conditioning of the Be limiter, which led to a strong reduction of Cl, the limit was substantially extended beyond that with Be gettering, so that $nRq_\psi/B_t \approx 33$ was reached with combined heating, ICRH and NBI heating. Furthermore the limiting density increases with the applied power as we shall see shortly. Pellet fuelled and He discharges have exceeded the deuterium gas fuelled limits. There is strong evidence that the edge density determines the limit. The limit at low q (q~2), however, is unchanged and is still set by major current disruptions.

There has not yet been such a systematic study for X-point discharges, but the behaviour is similar, with somewhat lower density limits. The highest densities so far in X-point discharges are obtained in H-modes with $nRq_\psi/B_t \approx 20\times10^{19}m^{-2}T^{-1}$. At higher densities, typically when $P_{rad}/P_t \approx 60\%$, an H to L- mode transition occurs and the density falls without causing a disruption. In limiter discharges the nature of the limit is different for C and Be limiters. With C, the limit is marked by an asymmetrical edge radiation (MARFE) that leads to a symmetric radiative collapse and ends in a hard disruption. With Be limiters the limit is generally marked by the appearance of a MARFE which, in gas fuelled discharges, is accompanied by a fall in recycling and reduction in density. This typically leads to a soft density limit with a relaxation oscillation of density, radiation and MARFE near the limit. The internal inductance of the plasma during the MARFE generally did not increase, indicating that the plasma was not contracting significantly, as in the pure C limiter during the radiation collapse. This is consistent with the absence of strong MHD fluctuations and disruptions in the Be-gettered and limiter plasmas.

The line-averaged density could be substantially increased with pellet fuelling, providing the pellets penetrated deeply. The limit for both pellet and gas fuelled discharges can be unified by considering the edge density and the input power (Fig. 2). The dependence of the density limit

on the total power P_t and in particular on the radiation power balance in the edge region of the discharge has been suggested in a number of papers [2-5]. These models suggest that the limit should increase approximately as $P_t^{1/2}$. The MARFE limit for pellet and gas fuelled discharges does lie at the boundary of the existence region.

2. CONCLUSIONS: DENSITY LIMIT

Operation near the density limit in JET can be summarised as follows :

- The density limit for additionally heated discharges in JET, with Be limiters in clean conditions, exceeds $nRq_c/B_t = 33 \times 10^{19} m^{-2} T^{-1}$;
- The density limit in gas and pellet fuelled discharges increases with input power approximately as $P_t^{1/2}$ and is determined by edge parameters, particularly the edge density;
- Its radiative nature and the difference between C and Be walls make it clear that the limit is determined by impurity content and hence wall interaction and material type;
- The high limit obtained in JET means that acceptable densities should be reached in next step devices provided that sufficient degree of impurity exclusion can be obtained.

3. BETA LIMITS

High β operation has been achieved at low toroidal fields (B < 1.2 T) where the Troyon limit [6] is reached with additional heating at power levels ~10MW below that at which carbon self-sputtering becomes important [7]. It has not yet been possible to surpass the Troyon limit as has been done in DIII-D [8].

Fig.3 shows the maximum toroidal β_ϕ as a function of q_c^{-1} obtained for all discharges between 1986 and 1989. A steady state β_ϕ of 5.5% has been reached for DN H-modes in a hydrogen plasma. In these discharges with Be coated walls, β saturation is generally observed without disruptions. The saturation is related to MHD-modes, ELM's and n=1 activity. Sawtooth and fishbone events occur and sometimes continuous n=1, 2, or 3 modes appear, which can lead to a β decline. A peaked and roughly triangular p(r) profile develops from an initially broad profile. The internal inductance decreases from ~ 1 to 0.7, which indicates a broadening of j(r) towards those profiles used in the β-optimisation by Troyon [6]. The decrease of the inductance is calculated to be due to the bootstrap current, which is approximately 25% of the total current.

4. BETA SATURATION

The evolution of β for the discharge with the highest β obtained so far is shown in Fig.4. Also shown is the MHD activity, central ion temperature and volume-averaged density as a function of time. The main β-limiting mechanism in this discharge is the high-β sawtooth. Increased MHD (n=1 and n=3) activity (around t=15 s) leads to a diminished rate of rise in β after the crash and to a decline in the central ion temperature and so contributes to the β saturation.

The high-β sawteeth differ from those at low β in two ways :

1. The associated heat pulse is very rapid with τ_{HP}~100μs instead of ~10 ms.
2. Dominant (1,1), (2,1) and higher m pre- and postcursors are seen, similar to high-β fishbones but of twice the amplitude. The modes have a ballooning character near the outer edge with a ratio in amplitude from the low to high B-side of ~10 as seen by the X-rays. Similar to a normal sawtooth, a high-β sawtooth causes a flattening of the pressure profile within the q=1 radius.

5. HEAT LOSSES

Like other H-mode discharges in JET the high-β discharge has a confinement time twice that of the Goldston L-mode [9]. The observed plasma energy W_{DIA} lies close to the energy W_G calculated from the effective power input and $\tau_E = 2 \times \tau_G$ [10]. The fraction of the losses due to high β sawteeth is 10 to 15% and that due to the intermittently appearing MHD-modes 20 to 30%

of the total energy losses. This is sufficient to prevent further β increase since the heating power P is close to the critical power required to reach the Troyon limit. The fishbones and especially the sawtooth events strongly affect the fast particle distribution as measured by the neutron emission with consequences for future α-particle heating.

The central neutron emission drops by 70 % (Fig.5) and its total rate by 30 % during a sawtooth [11]. Fishbones are observed which individually cause up to 10% drop in the global neutron emission. However they occur about 10 times more frequently than sawteeth and may contribute appreciably to the central loss of fast particles and energy. Relatively large heat losses (150 kW) have also been measured by the neutral particle analyser with losses that are proportional to the MHD mode amplitude. Measurements with a multi-channel O-mode reflectometer indicate that high frequency density fluctuations grow exponentially with β_N. The measurements are carried out between 3.9 and 4.1 m with frequencies ~130 kHz well above the n=1 MHD modes present; perhaps, indicating high-n ballooning-mode activity.

6. BETA COLLAPSE

In a few JET cases, high β collapses occur triggered or preceded by large n=2 (or sometimes n=1 or 3) MHD activity with δB~15 G at the edge, and differ from β-saturation in various ways [7]:

- a dominant (3,2) and other coupled n=2 modes are responsible as seen from SXR analysis,
- there is a drop in the electron density in contrast to the saturation due to the high β-sawteeth,
- the central ion temperature and the fast ions are not affected at first.

7. PLASMA STABILITY

The stability of the high-β discharges has been examined with various stability codes : ERATO [12], HBT [13], BALLOON [14] and FAR code [15]. These stability studies are discussed more fully in [16]. It is found that before a high-β sawtooth the central plasma over more than half its radius is close to or even above the marginal ideal ballooning stability threshold. The ideal n=1 internal kink is also found to be strongly unstable for $\beta_N \approx 1$ when $q_0 \leq 1$. This instability may be linked to the observed (1,1) instabilities which seem to cause the β-saturation. We have calculated the fast particle effects on the internal kink. It is found that at the β values reached, the fast particles can no longer stabilise the internal kink. The operation is outside the Porcelli-Pegoraro stable region in the $(\gamma_{MHD}, \omega_*, \beta_{ph})$ space with experimental values of (1.0, 0.5, 1.5) [17]. In addition, severe fishbone activity is expected in this regime, resulting from the coupling with high energetic beam ions above 40 keV. It is further found that in the cases where the β-collapse occurs internal modes of either n=2 or n=1 structure, appear to be responsible for the enhanced plasma losses. These modes have been simulated by the FAR code where the q-profile has been tuned to match the measured X-ray fluctuations over the plasma cross-section [16]. In the case where n=1 modes are dominant, the q-profile had to be relatively flat in the centre with $q(0) \approx 1.1$, supported by Faraday-rotation measurements.

8. CONCLUSIONS: BETA LIMIT

In low q discharges at high β, saturation of the plasma energy is observed without disruptions. Global n=1 modes in the form of high-β sawteeth and fishbones are generally responsible for this saturation. Occasionally, β-collapses occur which seem to be related to large n=2 (some- times n=1 or 3) MHD modes. Triangular temperature profiles exist at the limit, which together with the rather flat density profiles lead to constant ∇p across the plasma. Such peaked pressure profiles are favourable for a fusion reactor. Both the fishbones and sawteeth strongly affect the fast particle distribution. This has important consequences for future α-particle heating, burn control and wall loading. The role of the ballooning limit in the inner part of the plasma is not yet clear. Generally good agreement between theoretically predicted internal modes and

observations at the beta limit, has been obtained. The role of the fast particles on the beta limit needs further study both theoretically and experimentally. Further experiments in JET are required to see if the beta limit remains a soft limit even at much higher input powers.

9. REFERENCES

[1] C.Lowry et al, Proc.17th Eur.Conf.on Contr.Fusion & Plasma Phys., Amsterdam (1990)
[2] J.Wesson et al. Nuclear Fusion **29**, 641 (1989)
[3] D.Campbell et al, Proc. 11th Int.Conf. on Plasma Physics and Contr. Nucl. Fusion Research, Kyoto, Nuclear Fusion Supp. (1987)
[4] A.Gibson, Nuclear Fusion,**16** (1976) 546.
[5] P-H.Rebut amd B.Green, Proc. 6th Int.Conf. on Plasma Physics and Contr.Nucl. Fusion Research, Berchtesgaden, Nuclear Fusion Supp. 1977
[6] F.Troyon, R.Gruber et al, Plasma Phys.& Contr. Fusion **26**(1984)209
[7] P.Smeulders et al, Proc.17th Eur.Conf.on Contr.Fusion & Plasma Phys., Amsterdam (1990)
[8] J.Ferron et al, Proc.17th Eur.Conf.on Contr.Fusion & Plasma Phys., Amsterdam (1990)
[9] R.Goldston, Proc.11th Eur.Conf.on Contr.Fusion & Plasma Phys., Aachen (1984)
[10] A.Gibson et al, Proc. 17th Eur.Conf.on Contr.Fusion & Plasma Phys., Amsterdam (1990), to be published in Plasma Phys. & Contr.Nucl.Fusion.
[11] F.Marcus et al, Proc.17th Eur.Conf.on Contr.Fusion & Plasma Phys., Amsterdam (1990)
[12] R.Gruber et al, Computer Phys. Commun. **21** (1981) 323
[13] J.P.Goedbloed,G.M.D.Hogewey et al, Proc.10th Int.Conf. on Plasma Phys.and Contr. Fusion, London 1984, IAEA (1985)165
[14] D.P.O'Brien, C.M.Bishop et al, Proc. 16th Eur. Conf. on Contr.Fusion and Plasma Phys., Venice (1989)
[15] L.A.Charlton et al, Journal Comp. Phys. **86**, 270 (1990)
[16] T.C.Hender et al, Proc.17th Eur. Conf. on Contr. Fusion & Plasma Phys., Amsterdam (1990)
[17] F.Porcelli et al, Proc.17th Eur.Conf.on Contr.Fusion & Plasma Phys., Amsterdam (1990)

Figure Captions

Fig.1 The operating density range for JET shown as normalised current $q_c^{-1} = \pi R I_p / 5 A B_\varphi$ [m,MA,m^2,T] versus normalised density $n_e R/B$ [10^{19}m^{-3},m,T]. Comparison is made between carbon disruptions (two broken lines at left) and MARFES with Be evaporation (solid symbols) and Be limiter (open symbols)

Fig.2. The normalised edge density versus input power showing that the MARFE density limit occurs at the boundary of the existence region close to the curve $n_{edge} R/B_\varphi = 2.37\ P_i^{1/2}$ [10^{19}m^{-3}, m, T, MW]. B_φ varies in the range 1.4 to 2.6 T.

Fig.3. The maximum toroidal beta ($\beta_\varphi = 2\mu_0 \langle p \rangle / B_\varphi^2$) as a function of q_c^{-1} (proportional to normalised current $I_p/B_\varphi a$[MA,T,m]), for all JET discharges with the poloidal beta $\beta_\theta > 0.4$. The line is the Troyon limit $\beta_{Troyon} = 0.028\ I_p/B_\varphi a$ [MA,T,m]. The highest β is 5.5%.

Fig.4. Evolution of β_φ, MHD-mode amplitude B_φ (top-left), H_α and magnetic field B_φ (bottom-left), ion temperature T_i, volume average density $\langle n \rangle$ (top-right) and injected power P_{NI}, radiated power P_{rad} for the 5.5 % β discharge, a 2MA Double-Null H-mode at 0.9T with 11MW 80kV D-injection into a H plasma. $T_e(0)$ and $T_i(0)$ of 3.5 and 6 keV were obtained in these low q discharges ($q_{95} \approx 2.2$ or $q_c \approx 1.6$) and κ of 1.8. Z_{eff} slowly increases in time from 1.3 and levels off at ~2.5. The confinement time $\tau_E = 0.35$ s.

Fig.5. Cross-sections of the plasma neutron emissivity before and after a beta crash. The central emission drops by 70%. The integration time is 100ms.

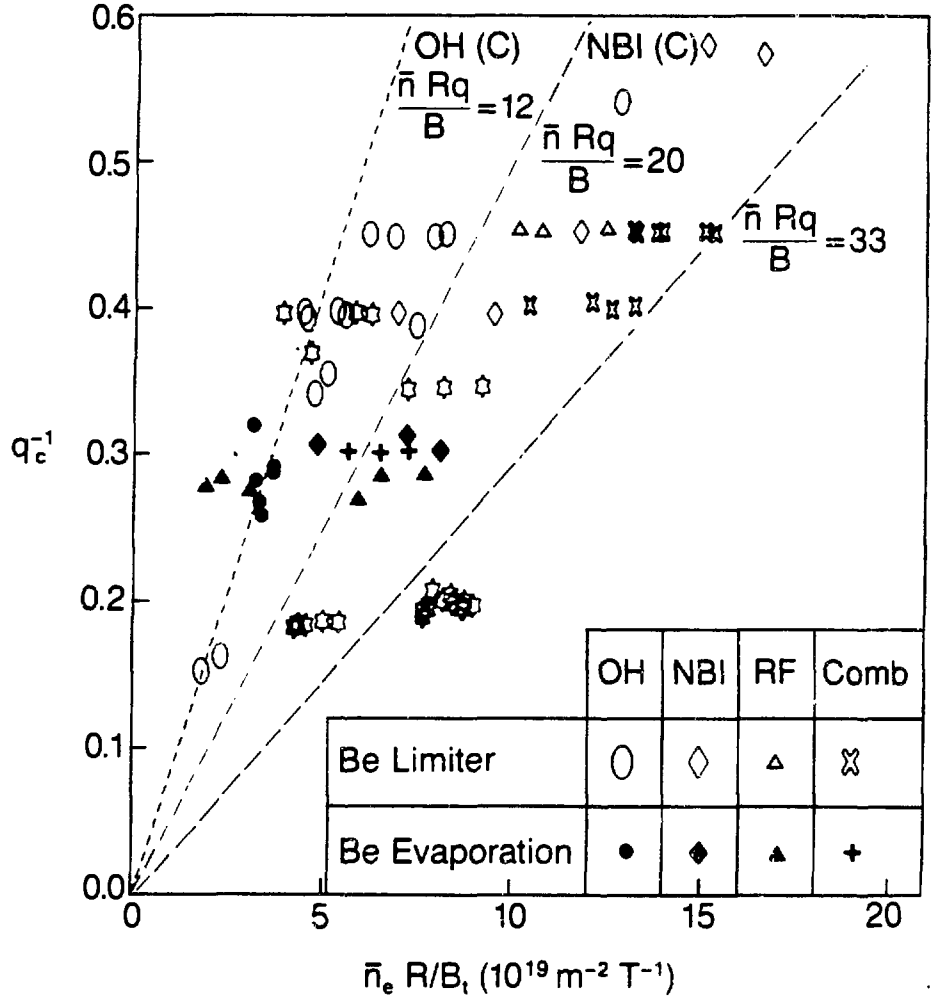

Fig.1 The operating density range for JET shown as normalised current $q_c^{-1} = \pi RI_p/5AB_\varphi$ [m,MA,m^2,T] versus normalised density n_eR/B [10^{19}m^{-3},m,T]. Comparison is made between carbon disruptions (two broken lines at left) and MARFES with Be evaporation (solid symbols) and Be limiter (open symbols)

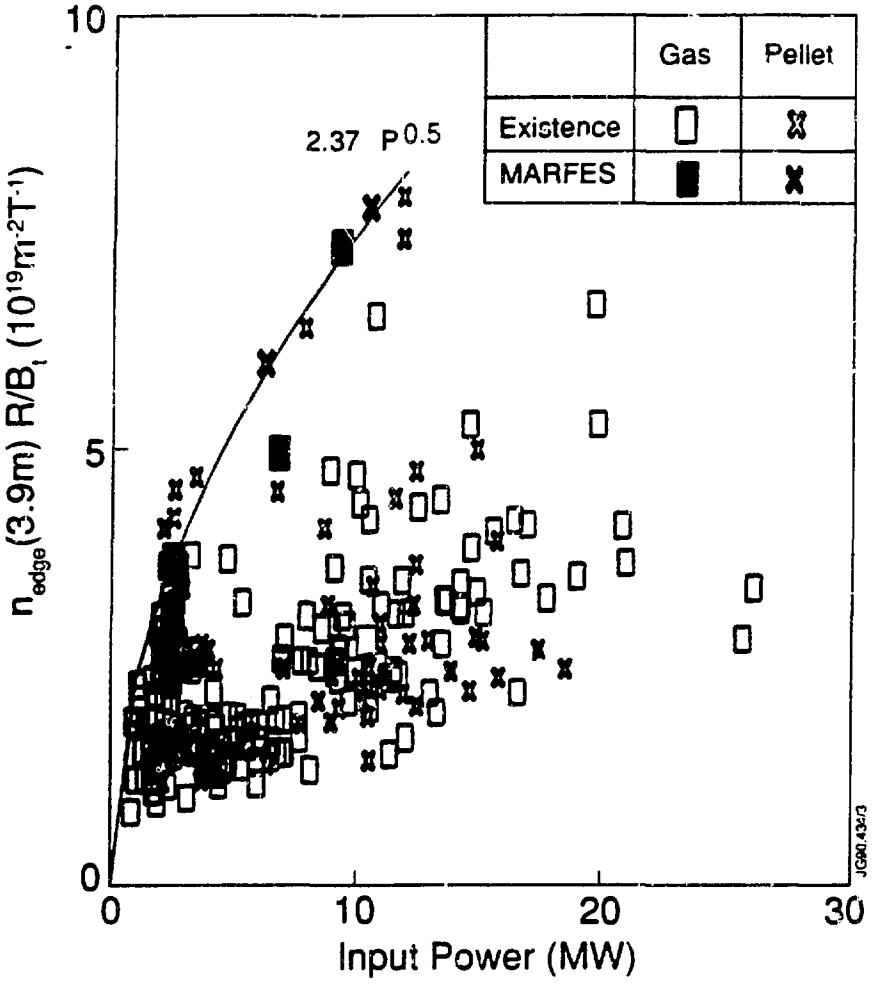

Fig.2. The normalised edge density versus input power showing that the MARFE density limit occurs at the boundary of the existence region close to the curve $n_{edge}R/B_\phi = 2.37\ P_t^{1/2}$ [10^{19}m^{-3}, m, T, MW]. B_ϕ varies in the range 1.4 to 2.6 T.

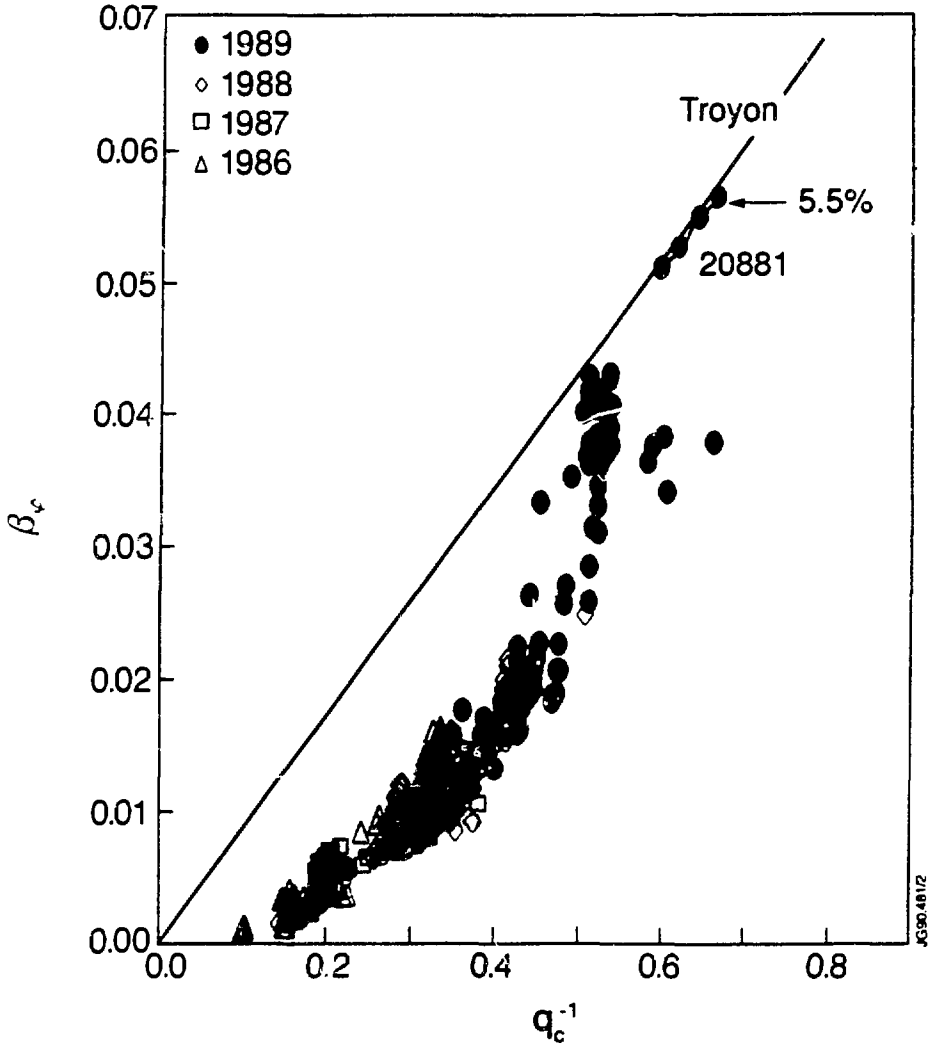

Fig.3. The maximum toroidal beta ($\beta_\varphi = 2\mu_0 \langle p \rangle / B_\varphi^2$) as a function of q_c^{-1} (proportional to normalised current $I_p/B_\varphi a$[MA,T,m]), for all JET discharges with the poloidal beta $\beta_\theta > 0.4$. The line is the Troyon limit $\beta_{Troyon} = 0.028\ I_p/B_\varphi a$ [MA,T,m]. The highest β is 5.5%.

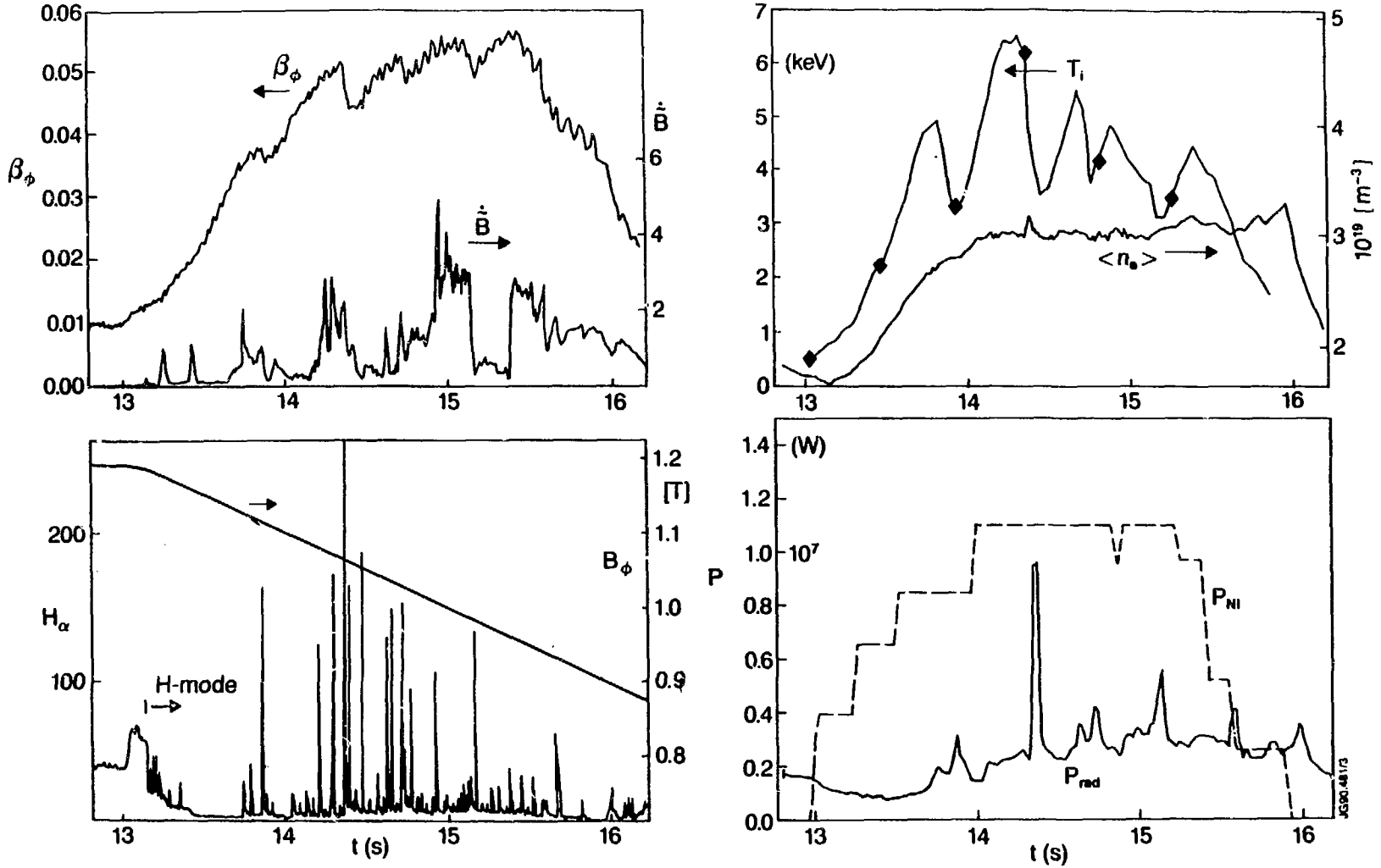

Fig.4. Evolution of β_φ, MHD-mode amplitude $\tilde{B}_\varphi$ (top-left); H_α and magnetic field B_φ (bottom-left); ion temperature T_i, volume average density $<n>$ (top-right); and injected power P_{NI}, radiated power P_{rad} for the 5.5 % β discharge, a 2MA Double-Null H-mode at 0.9T with 11MW 80 kV D-injection into a H plasma. $T_e(0)$ and $T_i(0)$ of 3.5 and 6 keV were obtained in these low q discharges ($q_{95} \approx 2.2$ or $q_c \approx 1.6$) and κ of 1.8. Z_{eff} slowly increases in time from 1.3 and levels off at ~2.5. The confinement time $\tau_E = 0.35$ s.

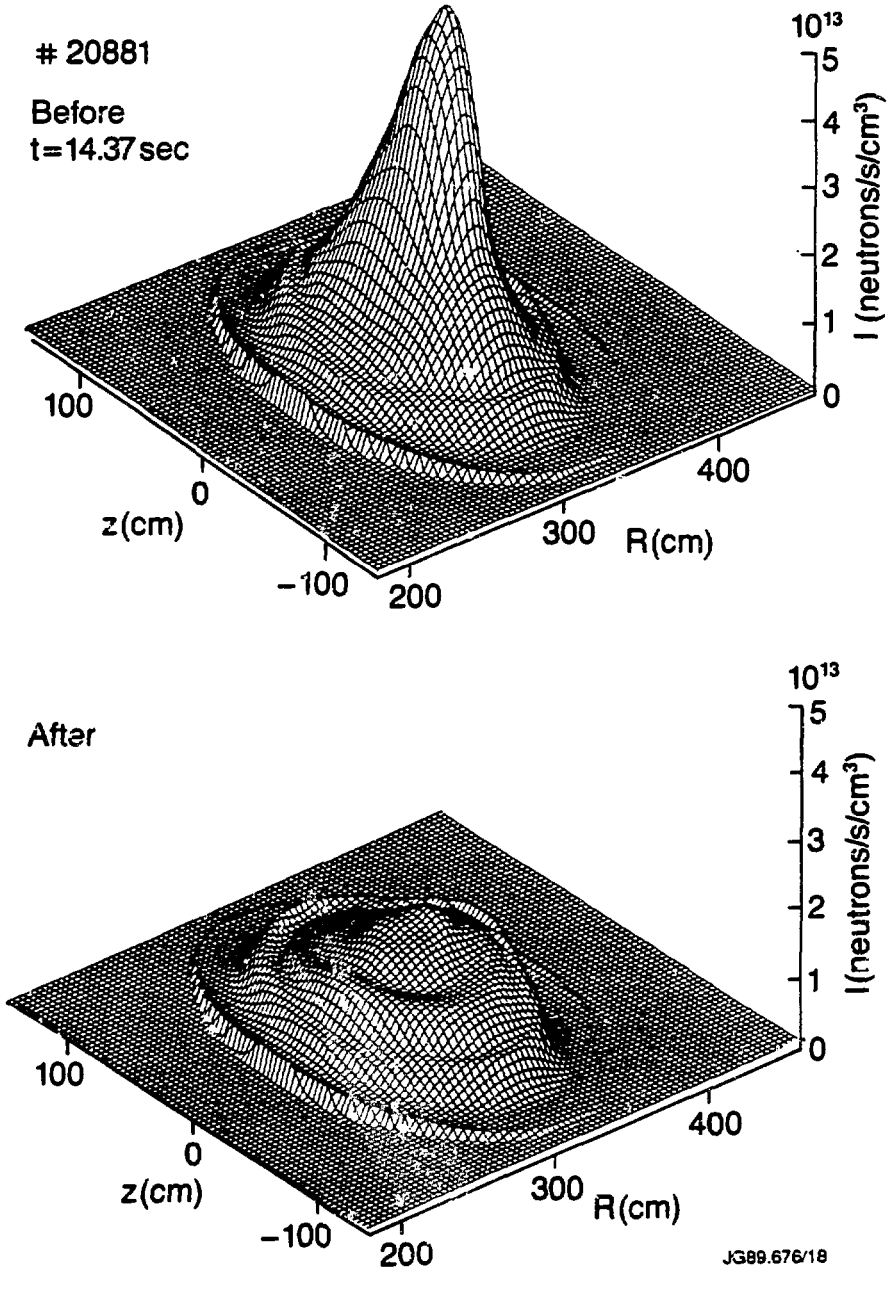

Fig.5. Cross-sections of the plasma neutron emissivity before and after a beta crash. The central emission drops by 70%. The integration time is 100ms.